

## Unusual thermal fatigue behaviors in 60 nm thick Cu interconnects

J. Zhang,<sup>a</sup> J.Y. Zhang,<sup>a</sup> G. Liu,<sup>a</sup> Y. Zhao,<sup>a</sup> X.D. Ding,<sup>a</sup> G.P. Zhang<sup>b</sup> and J. Sun<sup>a,\*</sup>

<sup>a</sup>State Key Laboratory for Mechanical Behavior of Materials and School of Materials Science and Engineering, Xi'an Jiaotong University, Xi'an 710049, China

<sup>b</sup>Shenyang National Laboratory for Materials Science, Institute of Metal Research, Chinese Academy of Sciences, Shenyang 110016, China

Received 21 June 2008; revised 16 September 2008; accepted 9 October 2008  
Available online 21 October 2008

Thermal fatigue of Cu interconnects 60 nm thick and 5–15  $\mu\text{m}$  wide was investigated by using alternating current to generate cycling temperature and strain/stress. The fatigue curves exhibit two regions, i.e. high- and low-cycle regions, which correspond to low and high thermal strains, respectively. The high-cycle region is found to be controlled by an unusual thermal fatigue mechanism of damage bands, which is related to a unique structure comprising only a single layer of grains distributed along the thickness.

© 2008 Acta Materialia Inc. Published by Elsevier Ltd. All rights reserved.

**Keywords:** Thermal fatigue; Thin films

Thermal fatigue is a potential reliability threat to interconnects that experience cyclic thermal strains during use [1,2]. Such cyclic thermal strains are usually induced by time-varying power dissipation (alternating current, AC) and the resultant time-varying temperature in the interconnects, because of the thermal expansion mismatch of the metal with the surrounding materials. AC-induced thermal fatigue in interconnects is a complex process involving electrothermomechanical coupling effects, which makes this fatigue behavior and mechanism much more complicated than those of pure mechanical fatigue and pure temperature-controlled thermal fatigue.

More concerns [3,4] are being raised concerning thermal fatigue in smaller interconnects of submicrometer or even nanometer size that are being used in the development of a new generation of integrated circuits. Recently, Mönig et al. [5] installed an apparatus directly in a scanning electron microscope to test the AC-induced thermal fatigue of metal interconnects; their approach enabled them to observe in situ the fatigue damage evolution. Using this new experimental method, Mönig et al. studied [5] the thermal fatigue of unpassivated 100 nm thick (average grain size  $d \sim 0.3 \mu\text{m}$ ) and 300 nm thick ( $d \sim 1.5 \mu\text{m}$ ) Cu lines and found that the fatigue damage was strongly dependent on the film thickness and grain

size. In the 300 nm thick Cu films with coarse grain, damage formation was found to be controlled by repetitive dislocation glide and to be localized in individual grains, just as observed in fatigued bulk metal samples. While in the 100 nm thick Cu films with relatively finer grains ( $d \sim 0.3 \mu\text{m}$ ), fatigue damage formation was found to be controlled by diffusion along boundaries and surfaces, because dislocation motion was hindered by the small volumes. These results roughly showed that the thermal fatigue of metal lines is also size dependent. The size-dependent mechanism in thermal fatigue is essentially similar to that observed in pure mechanical fatigue of metal films [6–8], i.e. from a dislocation-controlled mechanism to a diffusion-controlled one when reducing the length down to the submicrometer scale.

Following Mönig et al.'s work [5], more investigations have been carried out to study the influence of AC frequency [9] and interlevel materials [10] on the thermal fatigue damage of Cu interconnects. Raising the loading frequency was found [9] to accelerate damage formation and failure. The use of soft interlevel dielectric materials such as photoresist was revealed [10] to result in failure by hindering the formation of thermal fatigue damage on the Cu line surface. These results further indicate that thermal fatigue should be a serious threat to the reliability of devices when soft interlevel dielectric materials are used.

Although some progress has been achieved on the thermal fatigue of metal lines, many important issues

\* Corresponding author. E-mail: [junsun@mail.xjtu.edu.cn](mailto:junsun@mail.xjtu.edu.cn)

are still unclear, such as how the thermal fatigue behavior depends on the electrical current density and on the line width, and how the thermal fatigue will behave when the film thickness or grain size is reduced to even smaller dimensions. In this paper, 60 nm thick Cu lines 5–15  $\mu\text{m}$  wide are thermally fatigued in the AC density range from 3.2 to 26.5  $\text{MA cm}^{-2}$ . We first investigate the dependence of fatigue behavior or fatigue mechanism of Cu lines on the current density, especially at lower current densities, i.e.  $<10 \text{ MA cm}^{-2}$  where the mechanical part rather than the thermal and/or electrical one dominate the electro-thermomechanical coupling fields. In all the previous investigations [4,5,9,10], the thermal fatigue experiments were performed under high current densities, i.e.  $>10 \text{ MA cm}^{-2}$ , where the thermal or electrical part may be dominant. Secondly, the influence of line width on the thermal fatigue will be studied. A significant line width effect has been observed in the other two processes that affect the reliability of interconnects, i.e. electromigration [11–13] and stress-induced voiding [14,15]. It is thus believed that the thermal fatigue of interconnects should be also sensitive to line width. Thirdly, we will study the further size influence on the thermal fatigue when the film thickness is reduced down to 60 nm. The thinnest metal interconnect for which thermal fatigue has been reported is 100 nm thick Cu in Mönig et al.'s work [5], which was found to have a diffusive fatigue mechanism rather than dislocation slide. The thinner metal interconnects should therefore exhibit more interesting thermal fatigue behaviors and mechanisms.

Single-level test structures that have the same geometry as Mönig et al.'s sample [5] were fabricated using electron beam lithography, evaporation deposition and lift-off treatment.  $\langle 111 \rangle$  Si/SiO<sub>2</sub> wafers were first coated with photoresist and exposed to obtain the needed patterns by using a UV aligner (URE-2000). Cu films 60 nm thick were deposited onto the patterned substrates without a vacuum break using an evaporation system. After dissolving the photoresist using acetone, Cu line structures 1000  $\mu\text{m}$  long with widths of 5, 10 and 15  $\mu\text{m}$  were prepared. Figure 1a shows a typical optical image of the 15  $\mu\text{m}$  wide Cu line structure. All samples were annealed at 150 °C for 1 h in a high vacuum environment (less than  $10^{-8}$  mbar) to stabilize the microstructure.

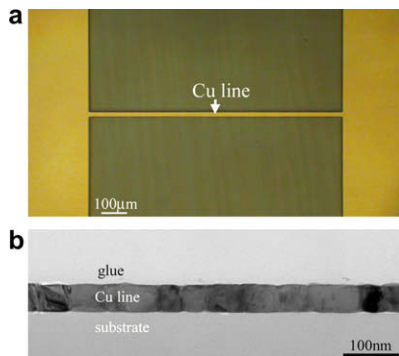


**Figure 1.** (a) The Cu line structure 60 nm thick and 15  $\mu\text{m}$  wide used in present thermal fatigue experiment. (b) A cross-section transmission electron microscopy image of the present Cu films showing a single layer of grains along the film thickness.

Grain size and microstructure of the Cu films were characterized by transmission electron microscopy (TEM). The mean grain size was determined to be about  $55 \pm 20 \text{ nm}$ , close to the film thickness. Only a single layer of grains was observed along the film thickness (Fig. 1b).

Thermal fatigue testing of the Cu interconnects was carried out in the chamber of a SEM by employing the method proposed by Mönig et al. [5]. Sinusoidal alternating voltages with frequency of 50 Hz were applied on the Cu interconnects to generate temperature cycles, resulting in cyclic thermal strain and thermal stress in Cu lines. Cycling temperature and temperature range  $\Delta T$  ( $\Delta T = T_{\text{max}} - T_{\text{min}}$ , where  $T_{\text{max}}$  is the maximum temperature and  $T_{\text{min}}$  is the minimum temperature at each cycle) of all testing lines at different current density were determined using time-resolved four-point resistance measurements. Subsequently, the strain range was obtained by the thermal strain  $\Delta \varepsilon = (\alpha_{\text{Cu}} - \alpha_{\text{Si}}) \Delta T$ , where  $(\alpha_{\text{Cu}} - \alpha_{\text{Si}})$  is the difference between the Cu and Si thermal expansion coefficients ( $\alpha_{\text{Cu}} = 17 \times 10^{-6}/^\circ\text{C}$ ;  $\alpha_{\text{Si}} = 3 \times 10^{-6}/^\circ\text{C}$ ). These strain cycles caused Cu lines to experience cyclic biaxial compressive–compressive strain, which induced thermal fatigue in the lines. The lifetime or the total number of cycles was recovered at the moment line failed. The applied current density ranged from 3.2 to 26.5  $\text{MA/cm}^2$ . At every current density, tested Cu line sample was fatigued to failure and at least three samples were used to ensure that the results were repeatable. The damage/failure morphology was observed in situ to analyze the thermal fatigue mechanism.

The cycling temperature, temperature ranges and the time to failure ( $t_f$ ) of lines was measured from a series of Cu lines at different  $j$ . The measured cycling temperature and temperature ranges are shown in Figure 2a and b, respectively. In Figure 2, every experimental dot corresponds to a tested Cu line. One can see from Figure 2 that the measured temperatures and temperature range are generally increased with increasing current density. This indicates that the density-dependent temperature (range) can be satisfactorily characterized in the present experiments and the temperature and strain range can also be regulated by adjusting the electrical current density.

The dependence of  $t_f$  on current density is plotted in Figure 3a. All three kinds of lines exhibit a similar trend, i.e. reducing  $t_f$  with increasing  $j$ . This can be easily understood because higher current density will cause a larger temperature range (see Fig. 2b) and thermal strain and thus accelerate the damage in lines. It can be also

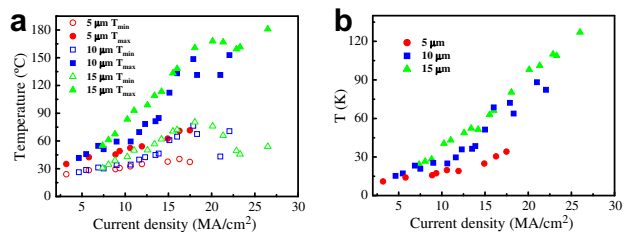


**Figure 2.** Measurements on the (a) maximum ( $T_{\text{max}}$ ) and minus ( $T_{\text{min}}$ ) temperature and (b) temperature range ( $\Delta T$ ) in the thermally cycled Cu lines with different line widths and different current densities.

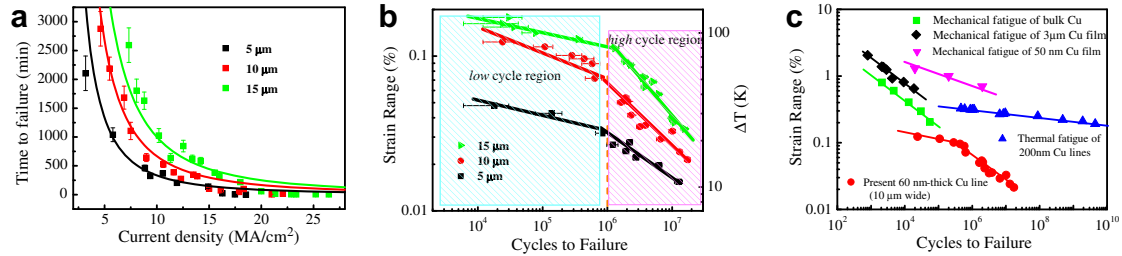


**Figure 3.** (a) Dependence of the time to failure of the Cu films on the line width as a function of current density. (b) Variation of lifetime ( $N_f$ ) with temperature range ( $\Delta T$ ) (right vertical axis) and strain range ( $\Delta \epsilon$ ) (left vertical axis) for different line widths. (c) Some previous results of mechanically fatigued 50 nm thick Cu film [17] (down triangle dots), 3  $\mu\text{m}$  thick Cu film [18] (diamond dots, average grain size 1.3  $\mu\text{m}$ ), thermally fatigued 200 nm thick and 8  $\mu\text{m}$  wide Cu line [10] (up triangle dots, average grain size 0.8  $\mu\text{m}$ ), and mechanically fatigued bulk Cu [19] (square dots, average grain size 55  $\mu\text{m}$ ) are also shown for comparison with the present thermally fatigued 60 nm thick and 10  $\mu\text{m}$  wide Cu line.

seen from Figure 3a that  $t_f$  is significantly sensitive to  $j$ . A significant line width effect can also be found in Figure 3a, i.e., the wider the Cu lines, the longer is  $t_f$ . For a given current density, the wider Cu lines have longer lifetime than the narrower ones. These results directly show that the thermal fatigue lifetime of Cu lines is also sensitive to the geometrical configuration, essentially similar to the other two failure fashions of electromigration [11] and stress-induced voiding [16]. The width effect is closely dependent on the thermal fatigue mechanisms, which will be described later.

The log–log treated thermal fatigue curves are also presented in Figure 3b, where the horizontal axis is the cycle to failure ( $N_f$ ) while the vertical axis is the average temperature range  $\Delta T$  (right axis) or corresponding strain range  $\Delta \epsilon$  (left axis) caused by  $j$ . It can be more clearly seen that the wider lines are able to bear a larger strain range at the same  $N_f$ . On the other hand, under the same strain range, the 15  $\mu\text{m}$  wide line is found to have the longest lifetime.

In Figure 3b, the fatigue lifetime is generally found to decrease with increasing strain range. One can also see that the  $N_f$  vs.  $\Delta \epsilon$  curves of all three lines show two similar regions. In the first region at somewhat low strain range,  $N_f$  decreases gradually with increasing  $\Delta \epsilon$ . This region is defined as the high-cycle region. With further increase in the strain range, the log–log  $N_f$  vs.  $\Delta \epsilon$  curves deviate from the first linear region and enter the second region, where  $N_f$  reduces sharply with increasing  $\Delta \epsilon$  and even down to only 3000 (0.5 min) at some much large  $\Delta \epsilon$ . This region is defined as the low-cycle region. The high- and low-cycle regions respectively correspond to the low and high strain ranges (or low and large  $j$ ).

Some previously reported  $N_f$  vs.  $\Delta \epsilon$  results are shown in Figure 3c, in comparison with present thermally fatigued 60 nm thick and 10  $\mu\text{m}$  wide Cu line. These results include those of mechanically fatigued 50 nm thick Cu film [17], 3  $\mu\text{m}$  thick Cu film (average grain size (AGS)  $\sim$  1.3  $\mu\text{m}$ ) [18], thermally fatigued 200 nm thick and 8  $\mu\text{m}$  wide Cu line (AGS  $\sim$  0.8  $\mu\text{m}$ , current density from 10 to 40  $\text{MA cm}^{-2}$ ) [10], and mechanically fatigued bulk polycrystalline Cu (AGS  $\sim$  55  $\mu\text{m}$ ) [19]. It is clearly found that, in pure mechanical fatigue, the size effect is significant, i.e. the thinner films have more fatigue resistance. However, when the films are subjected to thermal fatigue, the thermomechanical coupling effect causes the films to fail at much reduced lifetimes. For example, the

lifetime of the present thermally fatigued 60 nm thick Cu film is even less than that of the mechanically fatigued bulk Cu. The lifetime of Park et al.'s thermally fatigued 200 nm thick Cu film [10] is also longer than that of present 60 nm thick one. This may be related to the different interfacial bonding condition. Park et al.'s films were prepared by using magnetron sputtering and a layer of Ta was first deposited on the substrate before the Cu film deposition. However, the present Cu films were prepared by using evaporation deposition and were deposited directly on the substrate. This means that the present films may have weaker film/substrate interfacial bonding, which will result in inferior fatigue resistance.

From Figure 3c, one can see that the two-stage fatigue curve of the present Cu film is very different from all the other one-stage fatigue curves. The two-stage thermal fatigue behaviors of the present Cu lines are induced by distinct fatigue mechanisms respectively in the two stages. In the low-cycle region, the application of larger current density causes a very complex electrothermomechanical coupling field where the dominant influence of electrical and thermal parts accelerate the line failure.

In the high-cycle region, however, the current density is so low that the influence of mechanical part, rather than that of the electrical and/or thermal parts, will be dominant. This causes the damage morphology to be different from that observed in the low-cycle region. Figure 4a shows the typical damage morphology on fatigued Cu lines at  $j = 6.9 \text{ MA cm}^{-2}$  or  $\Delta \epsilon = 0.033\%$  for  $7.2 \times 10^6$  cycles (in the high-cycle region); damage bands are observed along the lines. Further microstructural analyses on the damage bands surprisingly revealed that

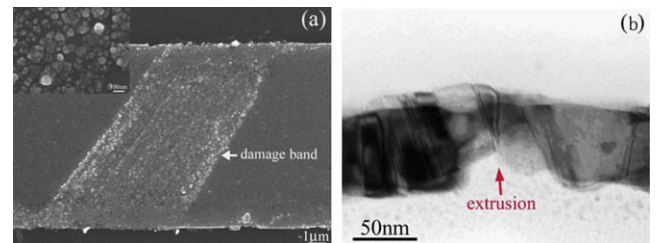


**Figure 4.** (a) SEM image showing the damage bands in the thermally fatigued 10  $\mu\text{m}$  wide Cu line at  $j = 6.9 \text{ MA cm}^{-2}$  or  $\Delta \epsilon = 0.033\%$  for  $7.2 \times 10^6$  cycles (in the high-cycle region). (b) A magnified image showing the damage bands formed by extrusion of grains. (c) TEM image showing the extrusion of grains.

the damage bands were caused by the extrusion of whole grains (Insert shows a magnified image taken within the damage bands in Fig. 4a). This was proved by cross-section TEM observations, as typically shown in Figure 4b where the grain indicated by the arrow can be clearly found to extrude out. This fatigue mechanism of grain extrusion is radically different from all the previous reports. A simple description on the fatigue mechanism of grain extrusion is as follows. In low current density regions or low cycling strain regions, damage is usually nucleated at the film/substrate interface because it is difficult to directly cause the nanograin films crack due to their high strength. Once local interface debonding is induced, current-enhanced grain boundary diffusion or interface diffusion will accelerate the interface debonding. Subsequently, the compressive–compressive fatigue will drive the fully debonded grains to extrude to form damage bands via grain boundary sliding.

This unique mechanically controlled and grain-boundary-sliding-aided fatigue mechanism of grain extrusion is exclusively associated with the present ultrathin and ultrafine films with a single layer of grains along the thickness. Although the fatigue in the high-cycle region is predominantly controlled by mechanical grain extrusion, it should be noted that the final failure of the films is still caused by electrical effects due to the gradual increase in localized resistance caused by extended damage bands.

Based on the above fatigue mechanism analyses, we can reasonably explain why the width dependence of thermal fatigue in the present experiments, i.e. the wider the line, the longer the lifetime, is somewhat different from previous reports. This is mainly related to the different length scales and the different fatigue mechanisms. In previous experiments (e.g. [4,5,9,10]), all the Cu lines have micrometer or submicrometer sized grains. At this length scale, repetitive dislocation slide within grains induces parallel surface wrinkling, where damage is nucleated and further propagated under thermal effects [4,5]. This thermal fatigue process is controlled by the dislocation action. Refining grain size could suppress the dislocation movement and delay damage nucleation, which is the reason why the 100 nm thick Cu lines have a longer fatigue lifetime than the 300 nm thick ones because the former have finer grains [5]. In the present experiments, however, the grain size of Cu lines is only about 55 nm, independent of width within the studied range. The damage nucleation in both the high-cycle and the low-cycle regions is much less affected by the line width. Damage propagation is controlled by the extension of damage bands along the line width and length. Within the studied range, the process of damage propagation will be prolonged in wider lines. This damage-propagation-dominated fatigue mechanism is responsible for the present width effect that wider lines have longer lifetimes. The relative contributions of damage nucleation process and damage growth process to the total fatigue lifetime have been also discussed by Kraft and Arzt [11] in analyzing the width-dependent electromigration lifetime of metal lines.

In summary, we prepared 60 nm thick Cu lines with line widths and studied the thermal fatigue behavior in situ by SEM. The following conclusions can be drawn:

- (1) A significant line width effect has been found experimentally, i.e. the narrower lines have weaker resistance to thermal fatigue. This is mainly because that the damage nucleation in the present Cu interconnects is less affected by the line width while the damage propagation process will be prolonged in wider lines.
- (2) The thermal fatigue curves exhibit distinct two regions, i.e. a high-cycle region and a low-cycle region, corresponding to low and high current densities, respectively. In the high-cycle region, fatigue is found to be dominated by the mechanically controlled damage mechanism of grain extrusion.

This work was supported by the National Basic Research Program of China (Grant No. 2004CB619303). The authors also wish to express their special thanks for the support from the National Natural Science Foundation of China and the National Outstanding Young Investigator Grant of China. This work was supported by the 111 Project of China and Program for Changjiang Scholars and Innovative Research Team in University (PCSIRT) and Science and Technology Key Research Program from Ministry of Education of China under Grant No. 02182 & 03182.

- [1] M. Huang, Z. Suo, Q. Ma, *Acta Mater.* 49 (2001) 3039.
- [2] E. Philofsky, K. Ravi, K. Hall, J. Black, in: *Proceedings of the Ninth Annual Proceeding of Reliability Physics*, IEEE, 1971, p. 120.
- [3] R.R. Keller, R. Mönig, C.A. Volkert, E. Arzt, R. Schwaiger, O. Kraft, *Proceedings of the Sixth International Workshop on Stress-Induced Phenomena in Metallization*, American Institute of Physics, New York, 2002, p. 119.
- [4] R. Mönig, Y.B. Park, C.A. Volkert, *Proceedings of the Eighth International Workshop on Stress-Induced Phenomena in Metallization*, American Institute of Physics, New York, 2006, p. 147.
- [5] R. Mönig, R.R. Keller, C.A. Volkert, *Rev. Sci. Instrum.* 75 (2004) 4997.
- [6] G.P. Zhang, C.A. Volkert, R. Schwaiger, P. Wellner, E. Arzt, O. Kraft, *Acta Mater.* 54 (2006) 3127.
- [7] G.P. Zhang, C.A. Volkert, R. Schwaiger, P. Wellner, E. Arzt, O. Kraft, *J. Mater. Res.* 201 (2005) 20.
- [8] O. Kraft, P. Wellner, M. Hommel, R. Schwaiger, E. Arzt, *Z. Metallkd.* 93 (2002) 392.
- [9] Y.B. Park, R. Mönig, C.A. Volkert, *Thin Solid Films* 515 (2007) 3253.
- [10] Y.B. Park, R. Mönig, C.A. Volkert, *Thin Solid Films* 504 (2006) 321.
- [11] O. Kraft, E. Arzt, *Acta Mater.* 46 (1998) 3733.
- [12] M. Hauschildt, M. Gall, S. Thrasher, P. Justison, L. Michaelson, R. Hernandez, H. Kawasaki, P.S. Ho, *Appl. Phys. Lett.* 88 (2006) 211907.
- [13] J. He, Z. Suo, T.N. Marieb, J.A. Maiz, *Appl. Phys. Lett.* 85 (2004) 4639.
- [14] J.H. An, P.J. Ferreira, *Appl. Phys. Lett.* 89 (2006) 151919.
- [15] D. Ang, C.C. Wong, R.V. Ramanujan, *Thin Solid Films* 515 (2007) 3246.
- [16] H. Okabayashi, *Mater. Sci. Eng. R* 11 (1993) 191.
- [17] D. Wang, C.A. Volkert, O. Kraft, *Mater. Sci. Eng. A* (2007), doi:10.1016/j.msea.2007.06.092.
- [18] O. Kraft, R. Schwaiger, P. Wellner, *Mater. Sci. Eng. A* 919 (2001) 319.
- [19] H.L. Huang, N.J. Ho, *Mater. Sci. Eng. A* 293 (2000) 7.